

Preparation and Characterization of Silica Nanoparticles by Wet Mechanical Attrition of White and Yellow Sand

Magda A Akl^{1*}, Hesham F Aly², Hesham M A Soliman³, Aref M. E. Abd ElRahman³ and Ahmed I. Abd-Elhamid³

¹Chemistry Department, Faculty of Science, Mansoura University, Mansoura, Egypt

²Hot Laboratories Center, Atomic Energy Authority, 13759, Egypt

³Advanced Technology and New Materials Research Institute, City for Scientific Research and Technology Applications, Borg El arab, P. O. Box 21934, Alexandria, Egypt

Abstract

Mechanical alloying is a simple and useful processing technique that is now being employed in the production of nanocrystals and/or nanoparticles from all material classes. In the present work, preparation of silica nanoparticles (SiO₂ NPs) by wet mechanical attrition of white and yellow sand using a lab scaled ball mill was investigated. The different experimental parameters affecting the milling process were thoroughly studied such as the milling period, water volume and the initial size of sand particles. Analysis of the results obtained revealed that SiO₂ NPs with particle size 22-33 nm and 38-48 nm could successfully be prepared from original white and yellow sand, respectively. The optimum experimental parameters to obtain these SiO₂ NPs are 25 g original sand particle, 50 ml water, 113 g media weight and 8 hr milling period at 400 rpm mill speed. The SiO₂ NPs obtained were characterized by SEM, XRD, EDS and FTIR. The results obtained showed high homogeneity of the produced spherical SiO₂ NPs. These SiO₂ NPs have good potentials for use in industry such as their use as additive materials in ultrahigh performance concrete for the next development. Based on economic value, the produced SiO₂ NPs have excellent potential to be developed.

Keywords: Nanosilica, attrition, SEM, XDR, EDS, FTIR

Introduction

Nanoparticles from mechanical attrition are produced by a “top-down” process, unlike nanoparticles produced from “bottom-up” processes such as self-assembly and template synthesis. These nanoparticles are formed in a mechanical device, generically referred to as a “mill,” in which energy is imparted to a coarse-grained material to effect a reduction in particle size. The resulting particulate powders can exhibit nanostructural characteristics on at least two levels. First, the particles themselves, which normally possess a distribution of sizes, can be “nanoparticles” if their average characteristic dimension (diameter for spherical particles) is less than 100 nm [1]. Second, many of the materials milled in mechanical attrition devices are highly crystalline, such that the crystallite (grain) size after milling is often between 1 and 10 nm in diameter. Such materials are termed “nanocrystalline” [2]. The sizes of the nanocrystals and the nanoparticles may or may not be the same. In some of the nanostructured materials literature, particularly that involving bottom-up processes, the term “nanocrystal” is reserved for crystalline particles with low concentrations of defects, such as are found in single crystals, whereas “nanoparticles” are those nanoscale particles that contain gross internal grain boundaries, fractures, or internal disorder, whether the crystals they contain are nanocrystalline or not [3].

The importance of nanoparticles lies in their inherently large surface-to-volume ratio relative to that of larger particles. These high surface areas can potentially improve catalytic processes and interfacially driven phenomena such as wetting and adhesion. Nanoparticles have the potential for use in structural and device applications in which enhanced mechanical and physical characteristics are required. As for the internal structure of the nanoparticles, it has been found that nanocrystalline materials have comparative advantages over their microcrystalline

counterparts in hardness, fracture toughness, and low temperature ductility [4,5]. As new methods for surface modification and post attrition processing of nanoparticles are developed, the potential applications for them continue to grow.

SiO₂ NPs are used in many industries such as semiconductor technology, optical communication, removal of heavy metals and dyes from water, catalysts, pigments and pharmacy industry.

SiO₂ NPs have been prepared by several techniques sol-gel process [6-12], microemulsion [13-16], oxidation of tetraethyl-orthosilicate TEOS in the bench-scale diffusion flame reactor [17], an interdigital micromixer and a batch reactor, have been used to prepare silica nanoparticles [18]. Recently, encapsulation of water insoluble drugs in mesoporous silica nanoparticles using supercritical carbon dioxide has been described [19].

A literature survey revealed that little information is available regarding the preparation of SiO₂ NPs by wet mechanical attrition of white and yellow sand. The aim of the present study is to throw light on the preparation and characterization SiO₂ NPs by wet mechanical attrition white and yellow sand based on their following peculiar properties: 1) they have mechanic strength to enhance the usable life. 2) The SiO₂ NPs possess nano-scaled size larger specific surface area allowing the easy adsorption of different environmental pollutants 3) the raw materials are low-cost and the synthetic approach is simple, which make these nanoparticles potentially commercializable.

In the present work SiO₂ NPs are obtained by wet mechanical attrition of white and yellow sand. The prepared SiO₂ NPs were characterized by SEM, XRD, EDS and FTIR. The different experimental

***Corresponding author:** Magda A Akl, Chemistry Department, Faculty of Science, Mansoura University, Mansoura, Egypt, Tel: 20-5022-42388 ; E-mail: magdaakl@yahoo.com

Received July 08, 2013; **Accepted** November 28, 2013; **Published** November 30, 2013

Citation: Akl MA, Aly HF, Soliman HMA, Aref ME, ElRahman A, et al. (2013) Preparation and Characterization of Silica Nanoparticles by Wet Mechanical Attrition of White and Yellow Sand. J Nanomed Nanotechnol 4: 183. doi:10.4172/2157-7439.1000183

Copyright: © 2013 Akl MA, et al. This is an open-access article distributed under the terms of the Creative Commons Attribution License, which permits unrestricted use, distribution, and reproduction in any medium, provided the original author and source are credited.

factors affecting the milling process were thoroughly investigated. The proposed method is particularly suitable for large quantity production, relatively simple with a few operation parameters, high homogenous product and low cost.

Materials

All chemicals were of analytical grade and used as received. All required solutions were prepared using de-ionized water, provided from a Milli-Q (Millipore, Bedford, MA, USA) purification system. White sand (S_{Si1}) was obtained from Suez Company for Minerals, Egypt. Yellow sand (S_{Si2}) was obtained from Borg Al-Arab desert. The two samples used without any further purification Analytical balance of type "Sartorius-GP 3202" was used to weight sand. A Vibratory Sieve Shaker of type "Retsch -AS200" basic was used for sieving of white sand. Milling of sieved white and yellow sand was performed using a "Retsch-PM400" planetary ball mill.

Preparations

Sieving of sand

100 gm of white or yellow sand was placed on a vibratory sieve shaker for 10 min at an amplitude of 100 mm. The sieving weight for each size fraction is given in Table 1.

Milling of white and yellow sand

25 gm of white or yellow sand was placed in a laboratory scaled ball mill. Samples were taken from a well mixed batch. Steel balls were used as milling media, steel veal was used as reactor and the ball mill was adjusted at 400 rpm on a "continuous mode". After every run, a certain amount of milled particles was suspended in an enough amount of double distilled water. A drop of the suspended particles was placed on a glass slide to dry on air to be characterized.

Characterization

Scanning Electron Microscopy (SEM): The surface morphologies of nanoparticles were investigated using scanning electron microscopy using Scanning Electron Microscopy (SEM) "Jeol Japan -JSM-636 OLA"

X-ray Diffraction Analysis (XRD): The crystallinity of particles was determined by X-ray diffraction (XRD) "Shimadzu, Japan XRD-7000"

Energy dispersive spectroscopy (EDS): The elemental analysis was achieved using SEM with EDS unit.

Fourier Transform Infrared Spectroscopy (FTIR): Various vibration modes were performed by Fourier transmission infra red spectroscopy (FTIR) "Shimadzu, Japan-8400s".

Results and Discussion

Milling of white sand

Effect of milling period: The influence of milling period on the

Size (μm)	Weight (gm)
2000-500	4.5
500-250	46.5
250-125	47.65
125-63	1.05
63-45	0.15

Table 1: The weight (gm) for each size (μm) of white sand after Sieving. (SiO_2 weight = 100gm Amplitude = 100mm time =10 min).

particle size of 25 g (150-250 μm) of S_{Si1} in 50 ml water using 113 g media weight and mill speed of 400 rpm was investigated. After 6 hr milling, the particle size of the dispersed silica particles was measured by SEM. At low magnification, 2500 X, large particles were observed in the range 0.57 to 2.37 μm , Figure 1 A (a & b). At higher magnification, 50000 X, SiO_2 NPs were observed in the range 23-38 nm. Under similar conditions and increasing the milling period to 8, 16 and 40 hr low magnification, large particles were not observed. At SEM with higher magnification, Figure 1B, C and D, the particle size in the range, 23-38 nm, at 8 hr, 32-58 nm, at 16 hr and 16-48 nm at 40 hr. The increase in the particle size at 16 hr is due to *reverse milling* [20]. Eight hours milling period was used for the subsequent milling processes. The relation between the milling period and the obtained SiO_2 NPs is represented in Figure 2.

Effect of water volume: Water was used as a wetting medium. The dependence of SiO_2 NPs on the water volume at milling period: 8hr, sand weight: 25 gm, media weight: 113 g and mill speed: 400 rpm was investigated. Figure 3 shows the low magnification 2500 X SEM of the particles obtained which indicates that with increase the volume of water from 0 to 25 ml the large particles break down into smaller particles with range particles size of 0.51-3.48 μm , 0.22-2.95 μm upon using 0 ml and 25, respectively. Further increase of the volume of water to 50ml the large particles disappear. At higher magnification, 50000 X SEM, the SiO_2 NPs were seen with average particles size of 22-51 nm, 22-47 nm and 23-38 nm upon using 0, 25 and 50 ml water, respectively. By addition of water the flow ability of the suspension was improved and there was, no longer, adherent particles to the wall of the vial nor the surface of the balls.

Effect of initial particle size of sand : The effect of initial sand particle size on the size of resulting SiO_2 NPs was investigated. Three samples, each 25 g, were subjected to milling: original sand sample, sample with size 125-250 μm and the third sample was in the range 250-500 μm . 25 g of each of the three samples was milled for 8 hr in 50 ml water using 113 g media weight and 400 rpm mill speed. The particle size obtained from each sample was compared with the particle size obtained from the original sample. It was observed that SiO_2 NPs of particle size, 22-30 nm, 25-38 nm and 23-38 nm can be obtained upon using sand of initial particle size between 500 -250 μm , 250 -125 μm and the original sand sample, respectively, Fig. 4. It can be concluded that the initial particle size has no effect on the size of the produced SiO_2 NPs. The relation between initial particle size and SiO_2 NPs is represented in Figure 5. 25 g of sand was used in all subsequent experiments.

Milling of yellow sand

The optimum conditions of the previous experimental factors (milling period: 8 hr, sand weight: 25 g, media weight: 113 g, water volume: 50 ml and mill speed: 400 rpm) were applied to yellow sand (S_{Si2}). The SEM images obtained, Figure 6 shows that SiO_2 NPs with size that ranged between 30-47 nm can be obtained by milling of yellow sand.

Characterization of SiO_2 NPs

XRD: Figures 7 and 8 show the XRD pattern of SiO_2 NPs of the milled white and yellow sand, respectively. Typical silica characteristic is observed with an intense sharp peak centered at $2\theta = 26^\circ$ which indicates that the samples are crystalline with crystal size 26.776 nm and 25.455 nm for the milled white and yellow sand respectively

EDS: The EDS of white and yellow sand before milling is represented

1.A) 6 hr

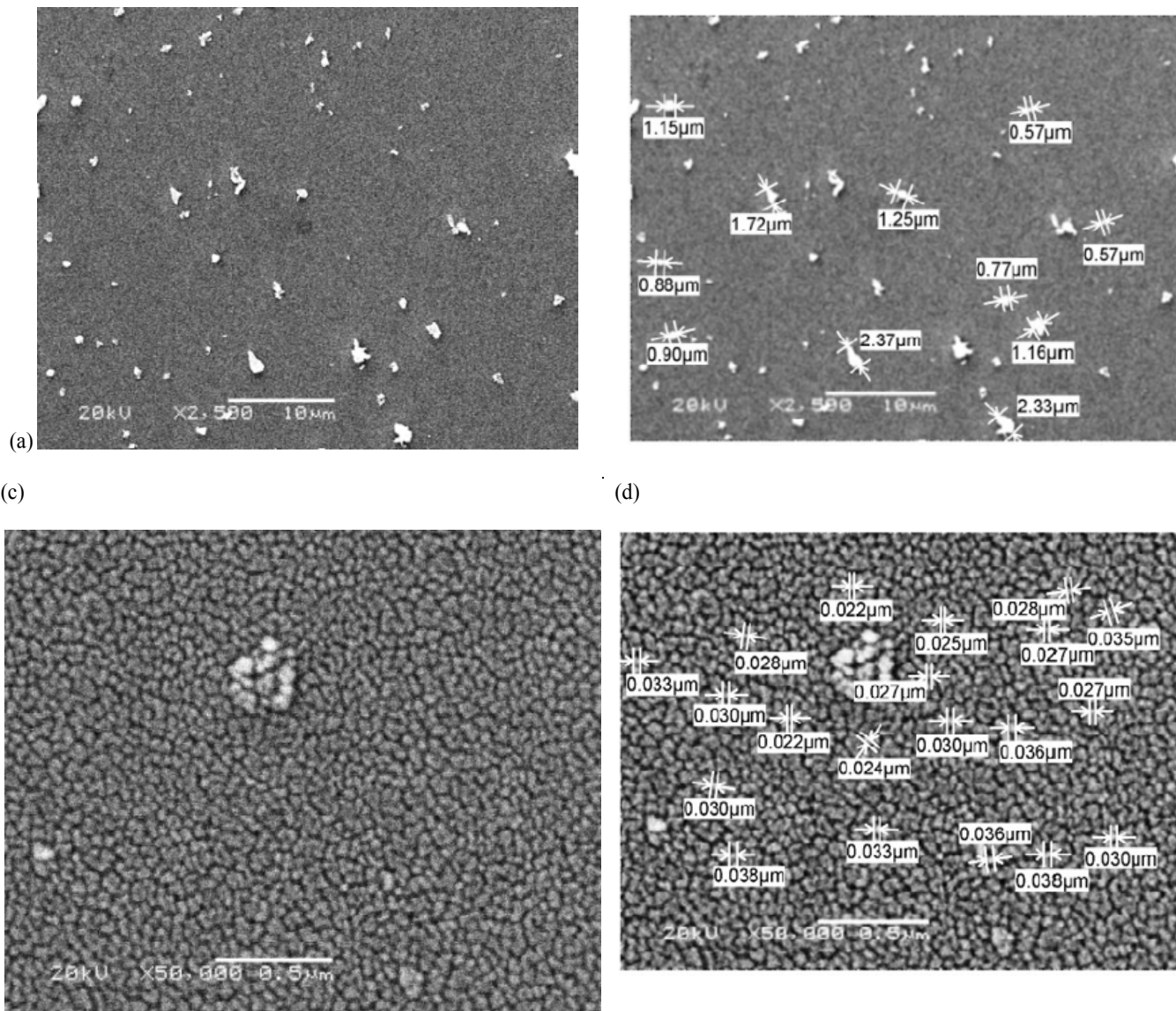


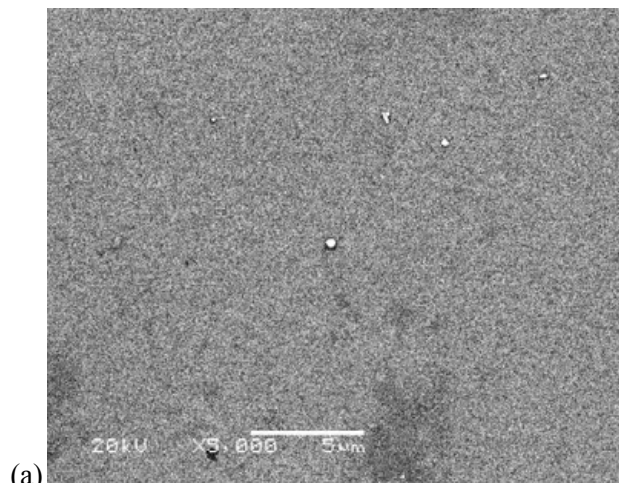
Figure 1a: SEM images of effect of milling period (hr) on SiO₂ NPs size (Sand weight: 25 g; Water volume: 50 ml; Media weight: 113 g; Mill speed: 400rpm; milling period 6 hr)

in Figures 9 and 10. The data of EDS of white and yellow sand before milling are shown in Tables 2, 3, respectively. The EDS measurements of the milled white and yellow sand show that the whole area of silica obtained was around stoichiometric composition (% At. Si = 32.90 and O = 66.30) and (% At. Si = 30.27 and O = 65.07), respectively, as shown in Figures 11 and 12, respectively. The iron appearing in the sample of white sand, Table 4, analyzed after milling insures that the sample was contaminated by iron from the stainless steel jar or the balls of the ball mill used. Also, the increase in iron content in SiO₂ NPs obtained from milling of yellow sand from 0.15% to 2.15, Table 5, can be attributed to the same reasons.

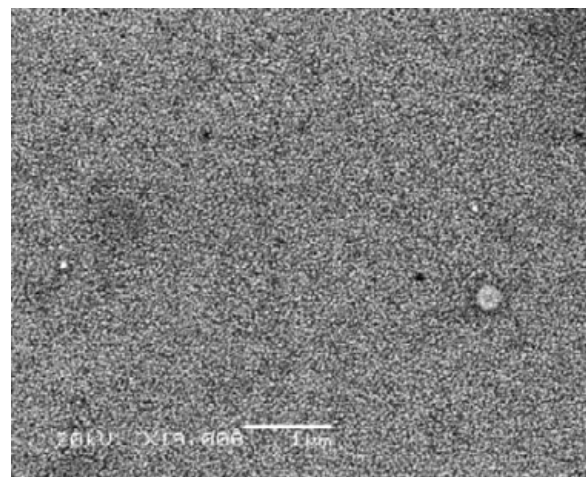
FTIR: The FTIR spectra of the silica obtained from the milling of

white sand and yellow sand Figures 13 and 14, show common bands assigned to various vibrations in the solid, respectively. The analysis of these spectra revealed the weak broad band centered at around 3440.77 cm⁻¹ for S_{Si1} and strong broad band centered at around 3435.95 cm⁻¹ for S_{Si2} to correspond to the overlapping of the O-H stretching bands of hydrogen-bonded water molecules (H-O-H...H) and SiO-H stretching of surface silanols hydrogen-bonded to molecular water (SiO-H...H₂O) [21]. The weak absorption band for S_{Si1} and The medium intense absorption band for S_{Si2} corresponding to the adsorbed water molecules deformation vibrations appear at 1615.27 and 1633.59 cm⁻¹, [22], respectively. The medium broad band at 1448.44 cm⁻¹ revealed to symmetric and asymmetric bending of C-H bond of -CH₂-CH₂- and very intense broad band at 1161.07 cm⁻¹ assigned to the longitudinal

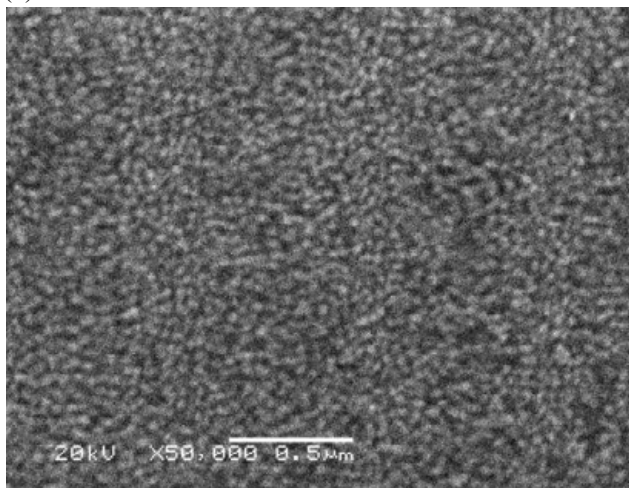
B) 8 hr



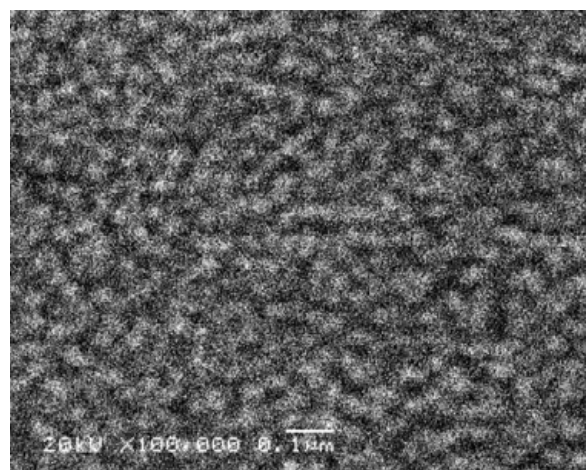
(b)



(c)



(d)



(e)

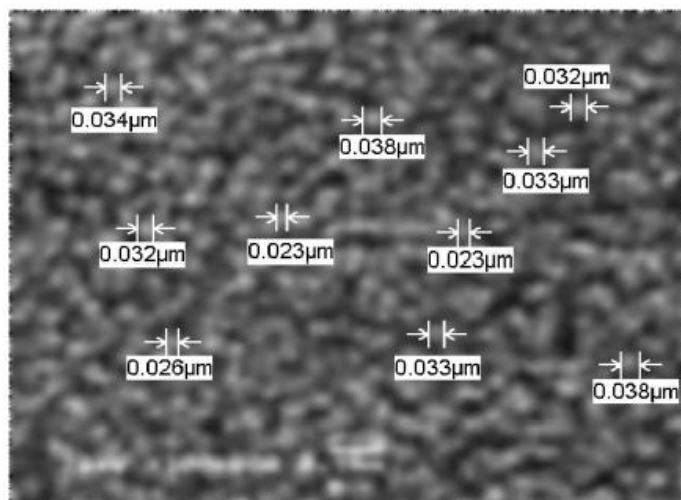
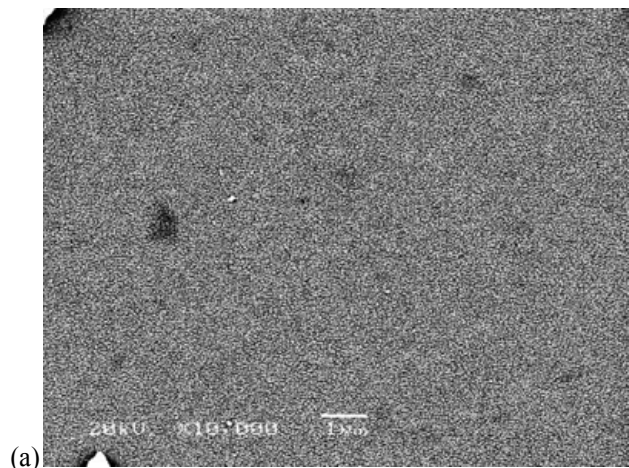
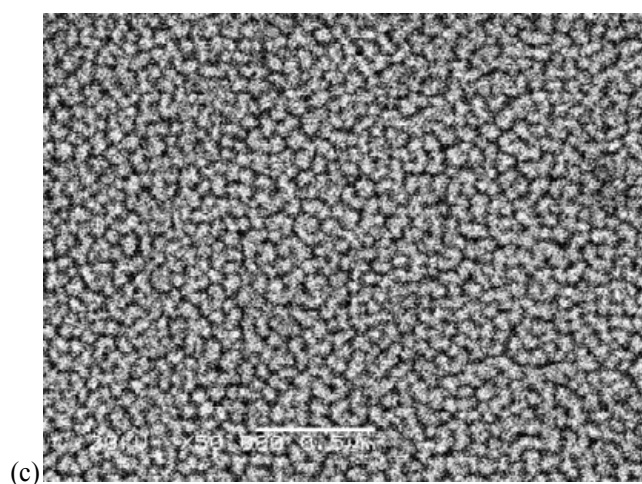
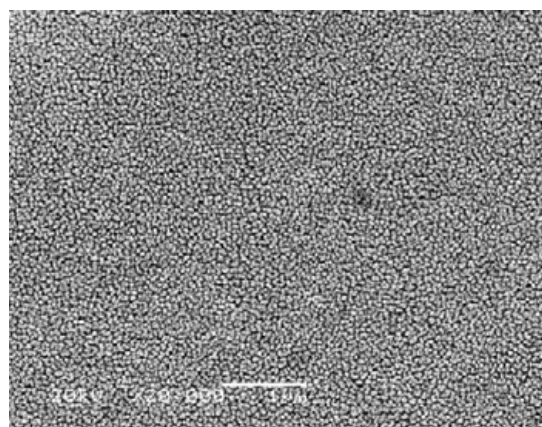


Figure 1b: SEM images of effect of milling period (hr) on the size of SiO₂ NPs (Sand weight: 25 g; Water volume: 50 ml; Media weight: 113 g; Mill speed: 400rpm; milling period 8 hr)

1. C) 16 hr



(b)



(d)

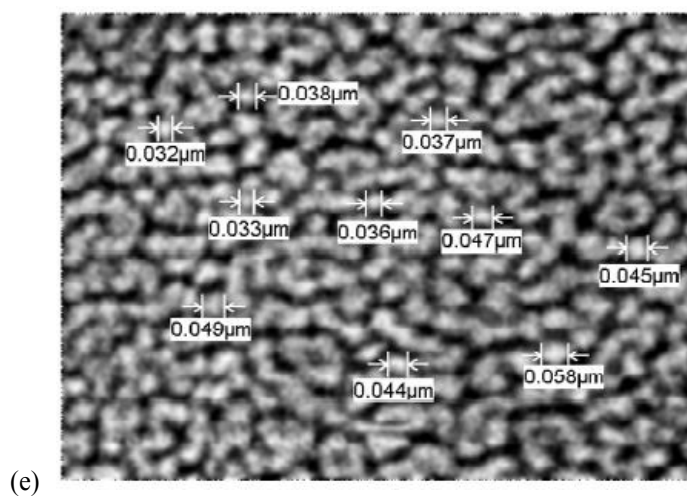
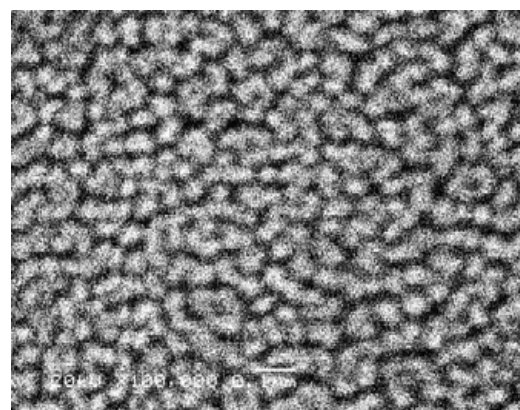


Figure 1c: SEM images of effect of milling period (hr) on SiO₂ particle size (Sand weight: 25 g; Water volume: 50 ml; Media weight: 113 g; Mill speed: 400 rpm; milling period 6 hr)

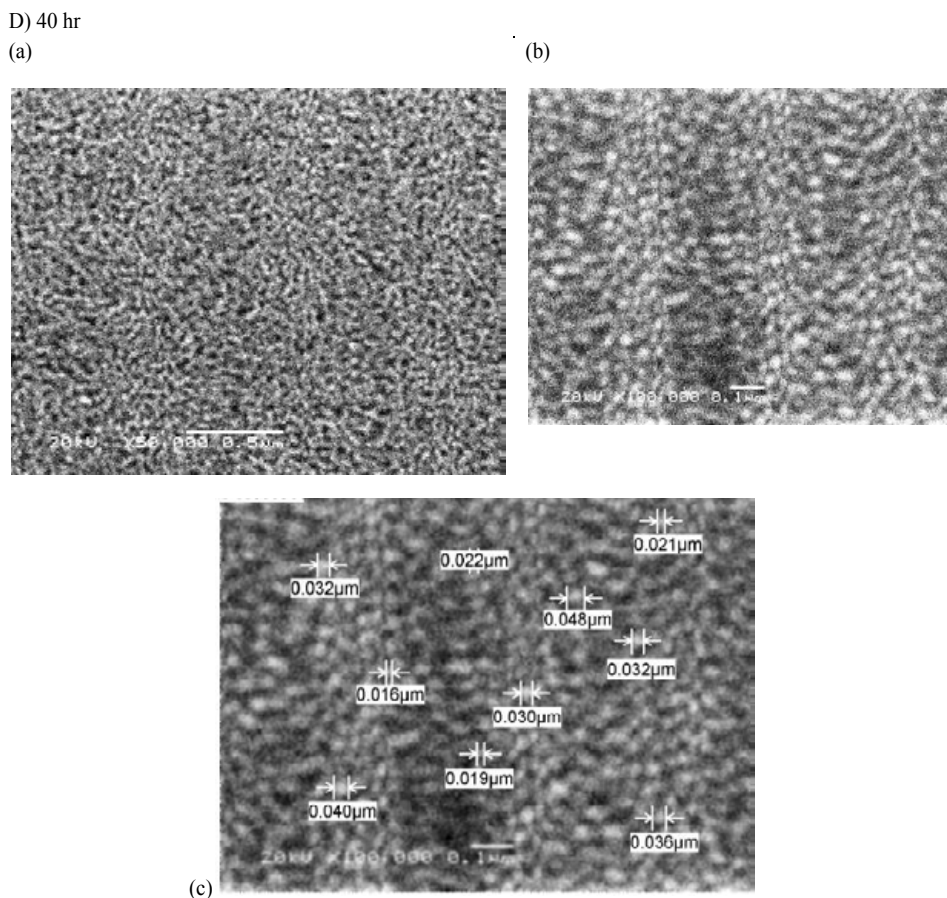


Figure 1d: SEM images of effect of milling period (hr) on SiO₂ NPs size (Sand weight: 25 g; Water volume: 50 ml; Media weight: 113 g; Mill speed: 400 rpm; milling period 6 hr)

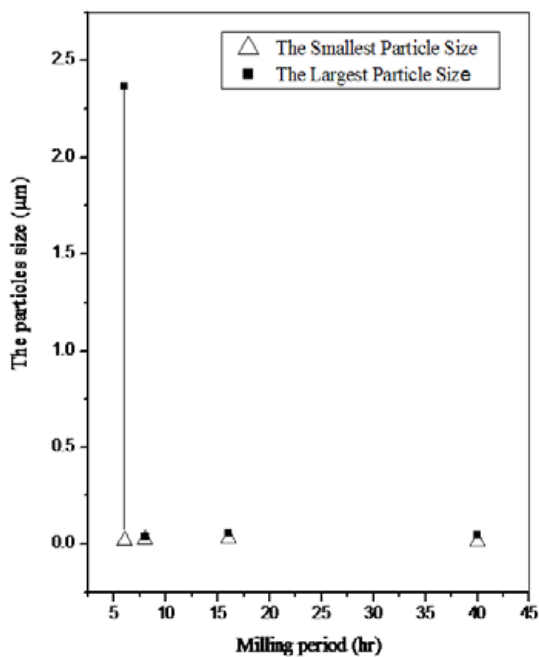


Figure 2: Effect of milling period on SiO₂ NPs (sand wt. 25 g, water volume 50 ml, media wt.113 g, mill speed 400 rpm)

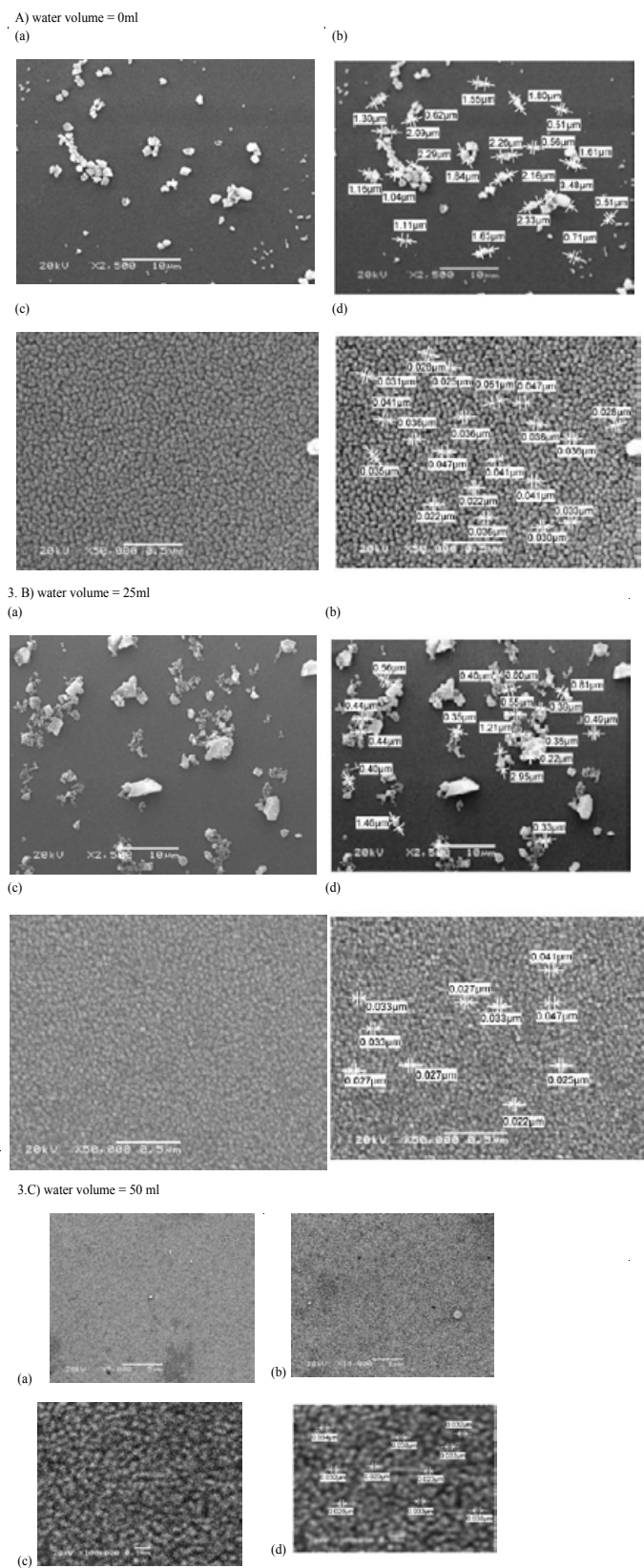


Figure 3: SEM images of effect of water volume SiO₂ NPs (Milling period: 8 hr, Sand weight: 25 g, Media weight: 113 g, Mill speed: 400 rpm.)
 A) Water volume = 0 ml, B) 25 ml and C) 50 ml

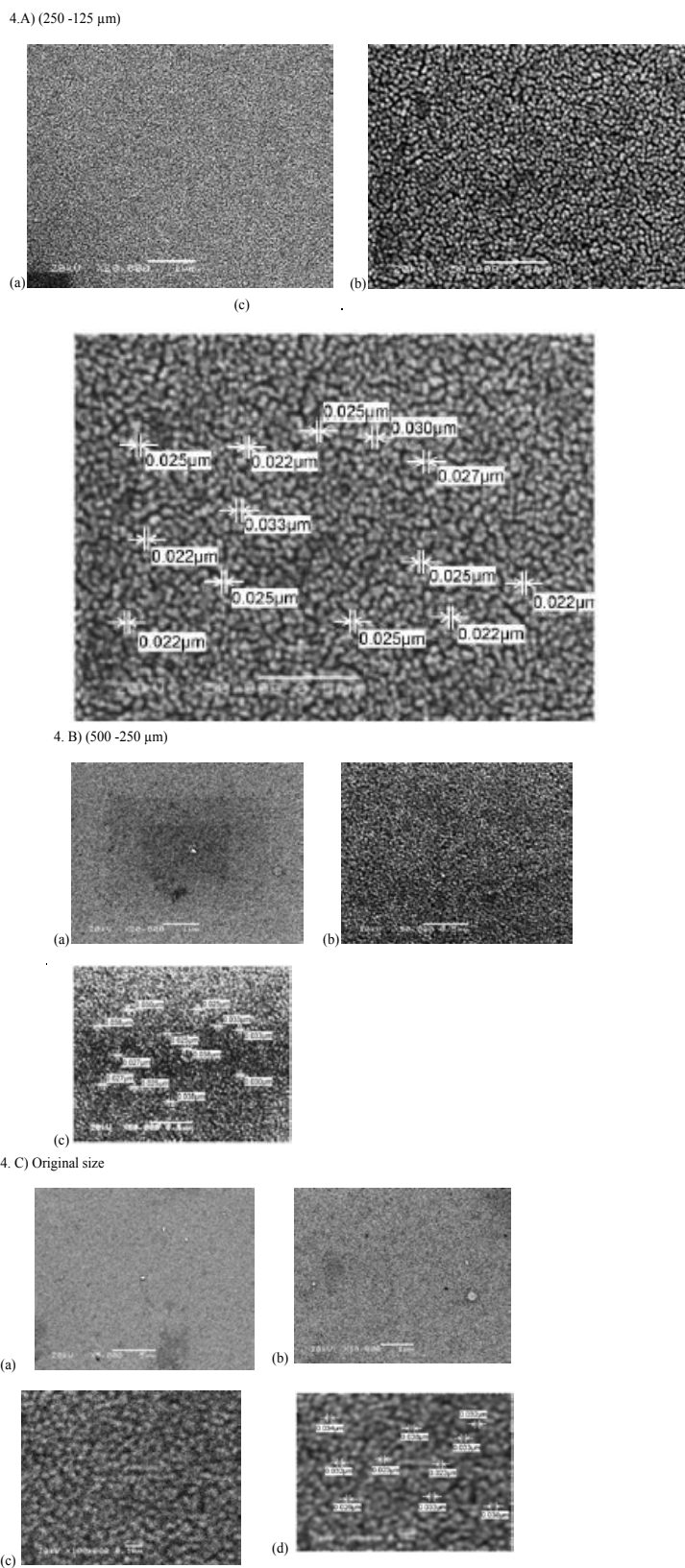


Figure 3: SEM images of effect of initial white sand particle size on the size of SiO_2 NPs, Milling period: 8hr, Sand weight: 25 g, Media weight: 113 g, Water volume: 50 ml, Mill speed: 400 rpm).
A) (250 -125 μm), B) (500 -250 μm) and C) original size

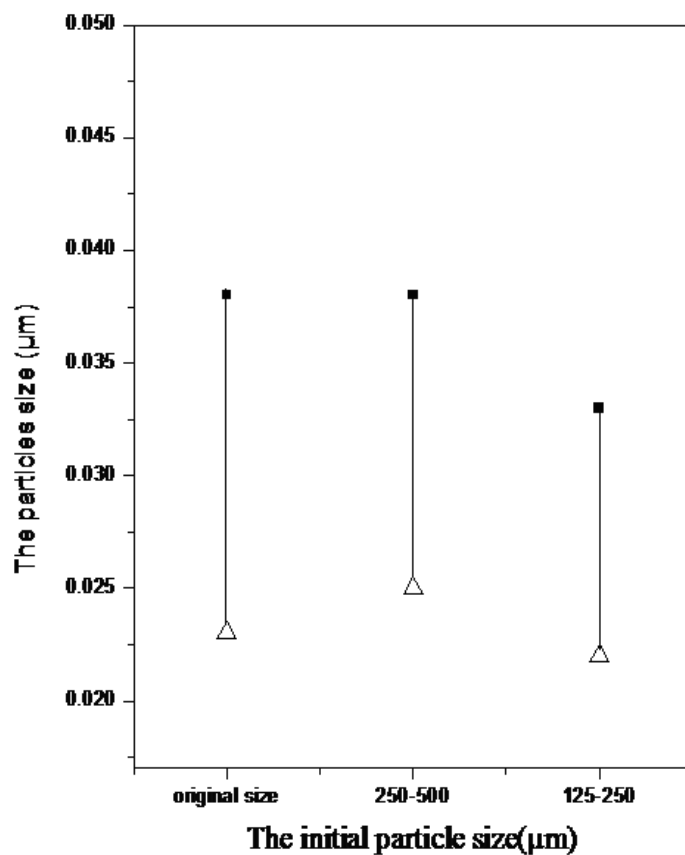


Figure 5: Effect of initial particle size on SiO₂ NPs (milling period 8 hr, water volume 50 ml, media wt.113 g, mill speed 400 rpm).

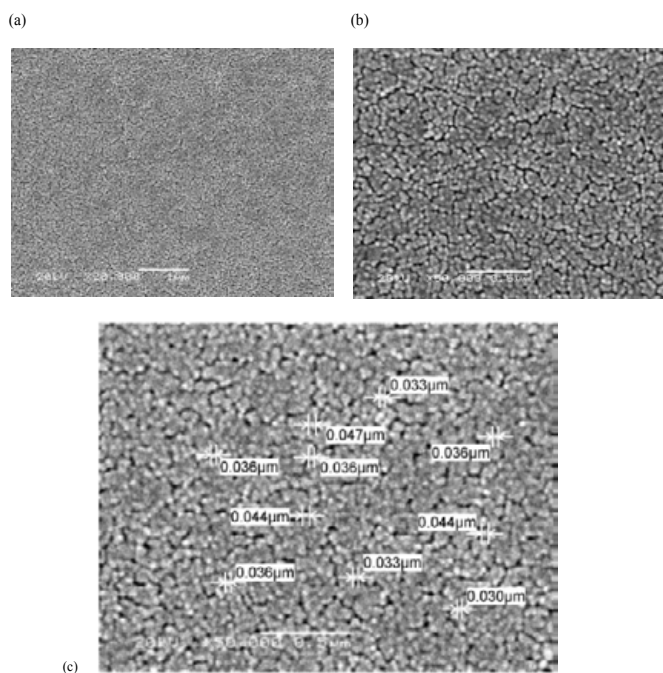
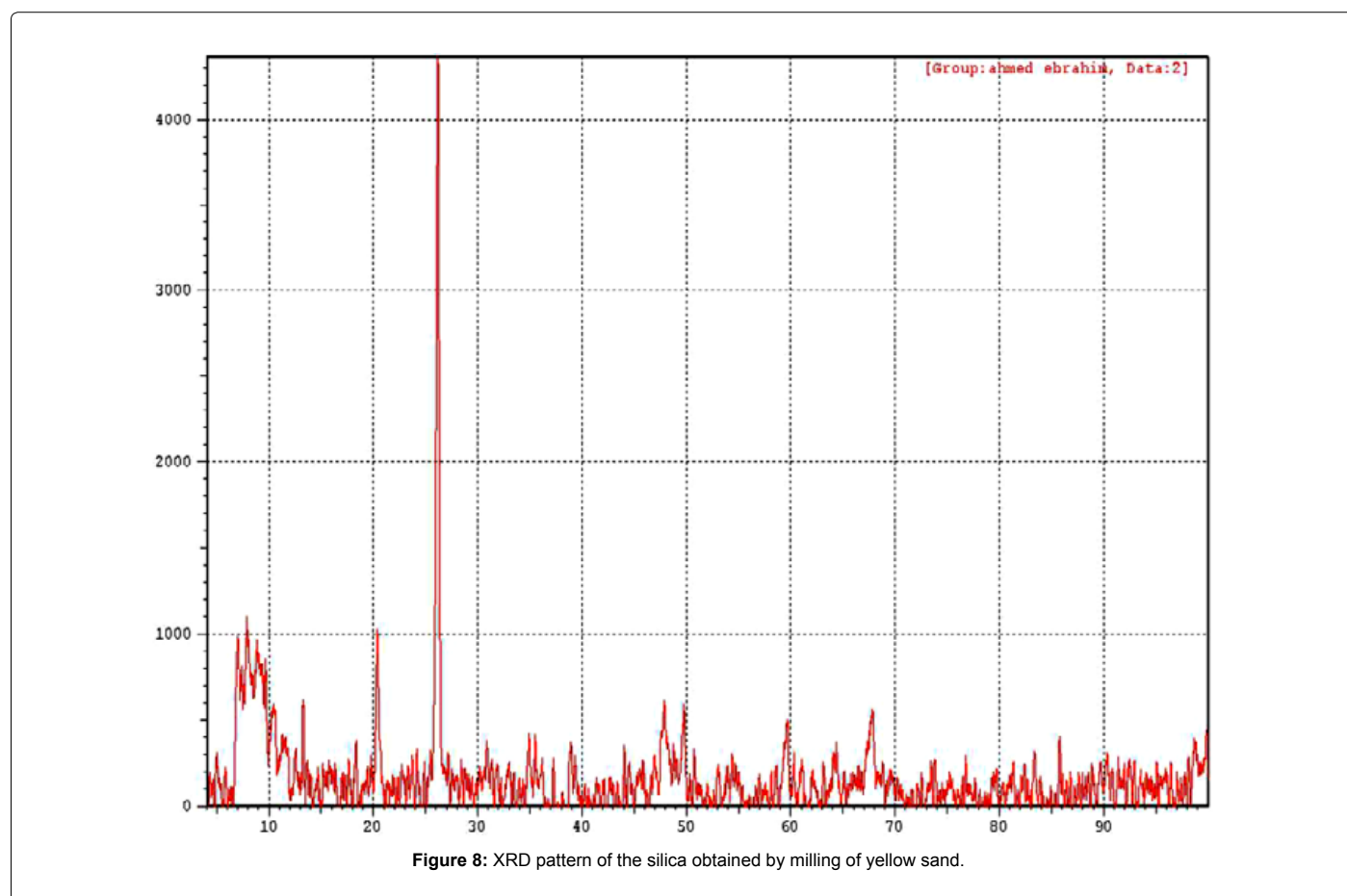
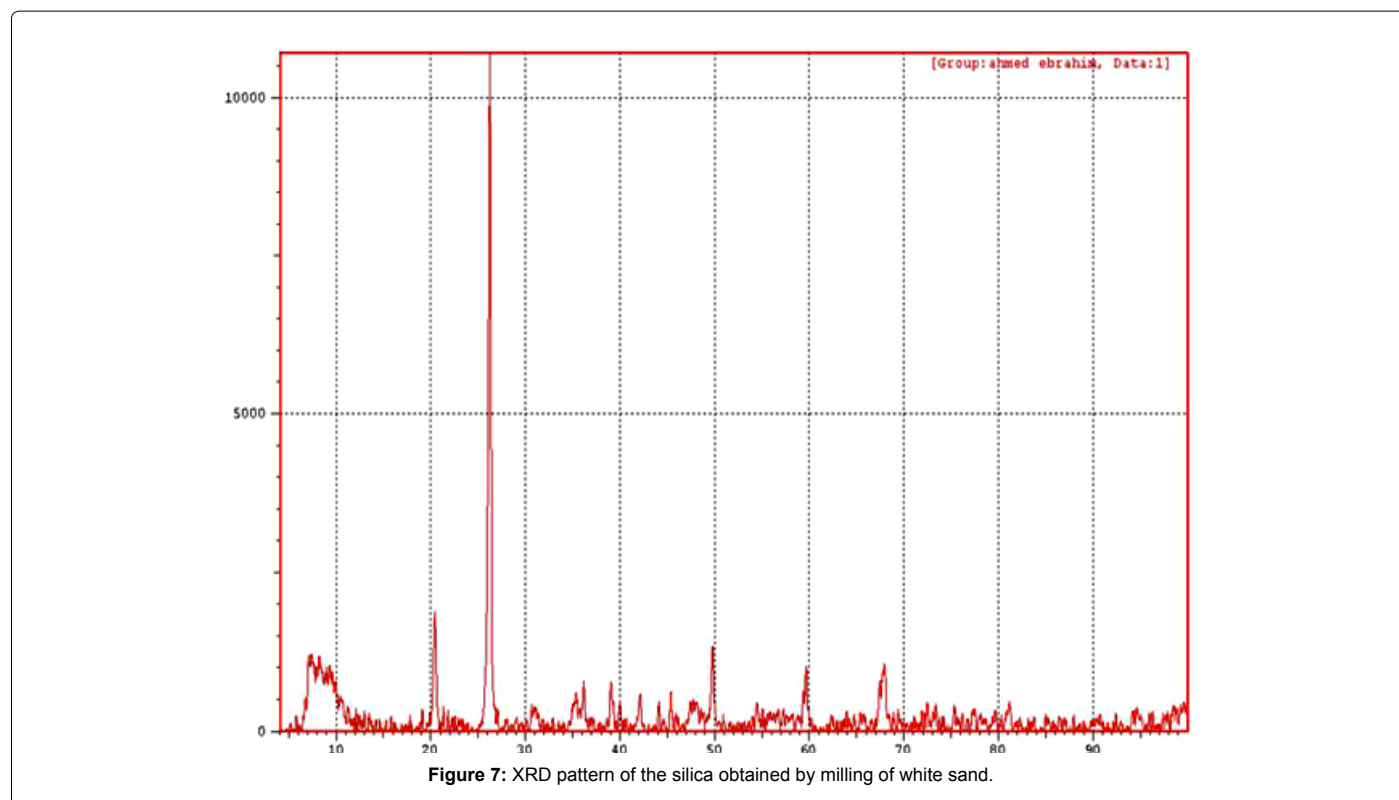


Figure 6: SEM images of the yellow sand particle size obtained at Milling period: 8 hr, Sand weight: 25 g, Water volume: 50 ml, Media weight: 113 g and mill speed: 400 rpm.



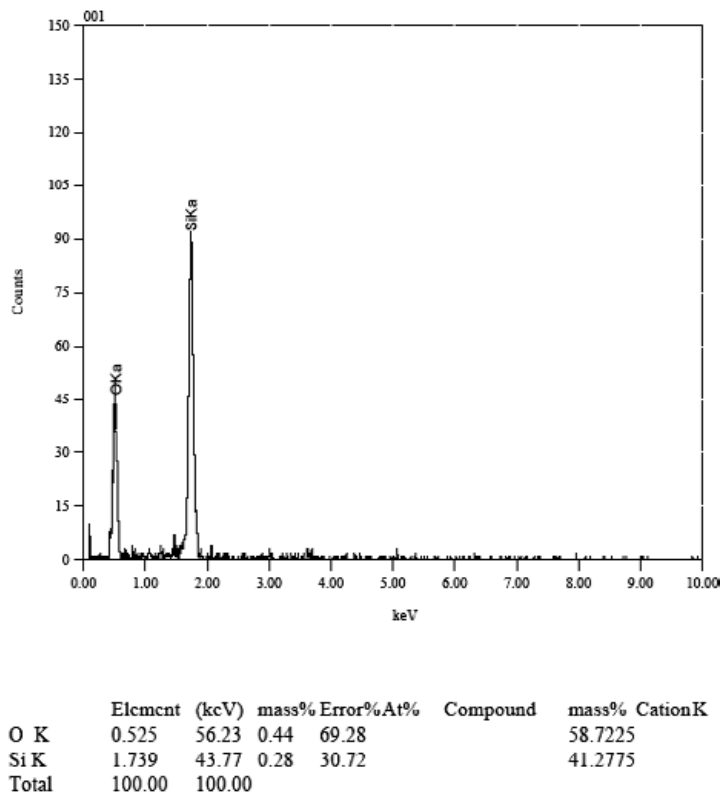


Figure 9: The EDS analysis for white sand before the milling.

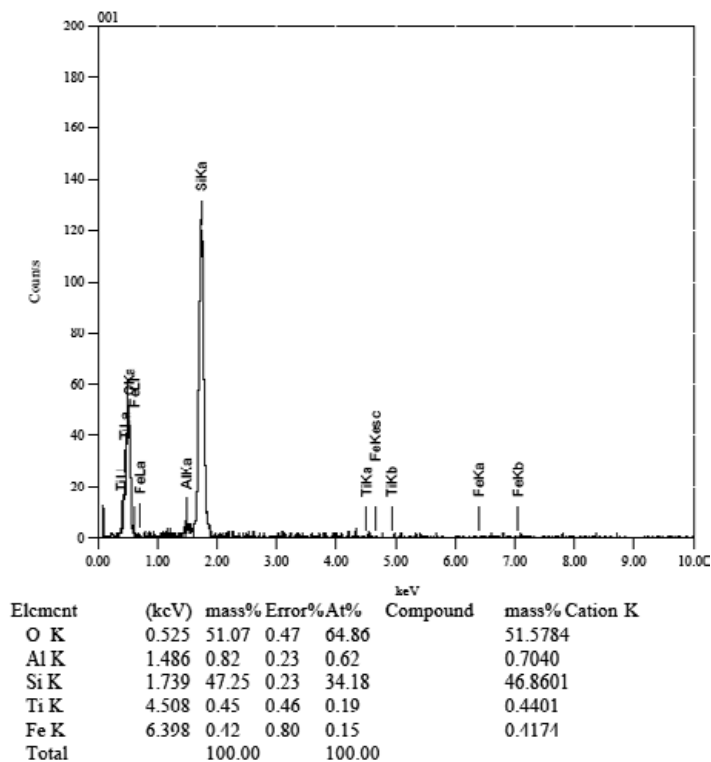


Figure 10: EDS analysis for yellow sand from Borg Al-Arab desert before milling.

Element	KeV	Mass%	Error%	At% compound	Mass % cation K
OK	0.525	56.23	0.44	69.28	58.7225
Sik	1.739	43.77	0.28	30.72	41.2775
Total		100.00		100.00	

Table 2: Elemental analysis of white sand before milling.

Element	KeV	Mass%	Error%	At% compound	Mass % cation K
OK	0.525	4	0.47	64.86	51.5784
AlK	1.486	0.82	0.23	0.62	0.7040
TiK	4.508	0.45	0.46	0.19	0.4401
Sik	1.739	43.77	0.28	32.90	43.7741
FeK	6.398	0.42	0.80	0.15	0.4174
Total		100.00		100.00	

Table 3: Elemental analysis of yellow sand before milling.

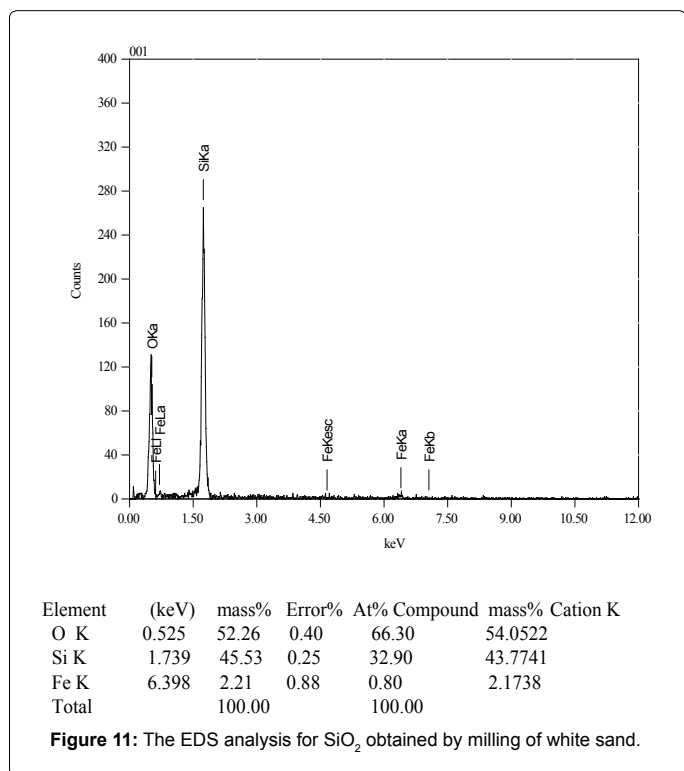


Figure 11: The EDS analysis for SiO₂ obtained by milling of white sand.

optical (LO) modes of the Si-O-Si asymmetric stretching vibrations [23] which found in S_{Si2} and absence in S_{Si1}. The very intense and broad band appearing at 1082.96 cm⁻¹ and 1083.92 assigned to the transversal optical (TO) modes of the Si-O-Si asymmetric stretching vibrations [23] for S_{Si1} and S_{Si2} respectively. On the other hand, the symmetric stretching vibrations of Si-O-Si appear at 785.94 cm⁻¹ and its bending mode appears at 459.63 cm⁻¹ and 479.28 cm⁻¹ [24] for S_{Si1} and S_{Si2} respectively. The weak shoulder band at around 698.63 cm⁻¹ and 692.40 cm⁻¹ for S_{Si1} and S_{Si2} respectively is assigned to Si-O stretching of the SiO₂ [25]. This difference in spectra between S_{Si1} and S_{Si2} may attributed to the impurities present in yellow sand such as Al and Ti.

Conclusion

Mechanical alloying is a simple and useful processing technique that is now being employed in the production of nanocrystals and/or nanoparticles from all material classes. Although a variety of mechanical alloying devices exist, the high-energy ball mill is typically used to

produce particles in the nanoscale size range. Particle size reduction is effected over time in the high-energy ball mill, as is a reduction in crystallite grain size, both of which reach minimum values at extended milling times.

Contamination from milling media (e.g., stainless steel vials and balls) is a serious problem that has not yet been thoroughly investigated. Despite these difficulties, MA is more widely used than ever and continues to be applied to the formation of nanoparticles and nanocrystalline structures in an ever-increasing variety of metals, ceramics, and polymers.

In the present work, SiO₂ NPs with particle size range of 23-38 nm were prepared by milling white and yellow sand in wet conditions using water as wetting agent for 8hr and 400rpm mill speed. The SiO₂NPs obtained are characterized using SEM, X-ray diffraction, EDS and

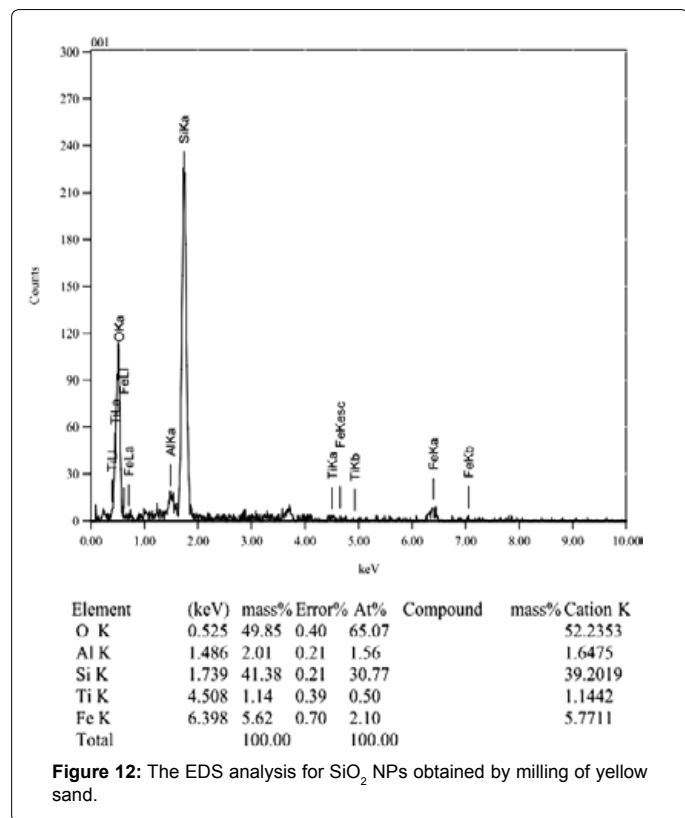


Figure 12: The EDS analysis for SiO₂ NPs obtained by milling of yellow sand.

Element	KeV	Mass%	Error%	At% compound	Mass % cation K
OK	0.525	52.26	0.44	66.30	54.0522
Sik	1.739	43.77	0.28	32.90	43.7741
FeK	6.398	2.21	0.88	0.80	2.1738
Total		100.00		100.00	

Table 4: Elemental analysis of white sand after milling.

Element	KeV	Mass%	Error%	At% compound	Mass % cation K
OK	0.525	49.85	0.40	65.07	52.2353
AlK	1.486	2.01	0.21	1.56	1.6475
TiK	4.508	0.45	0.46	0.19	0.4401
Sik	1.739	41.38	0.21	30.77	39.2019
FeK	6.398	5.62	0.70	2.10	5.7711
Total		100.00		100.00	

Table 5: Elemental analysis of yellow sand after milling.

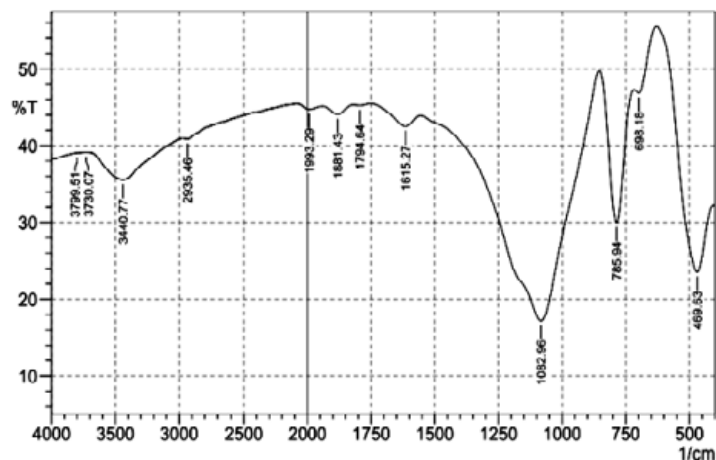


Figure 13: FT-IR spectra of SiO₂ NPs obtained by milling of white.

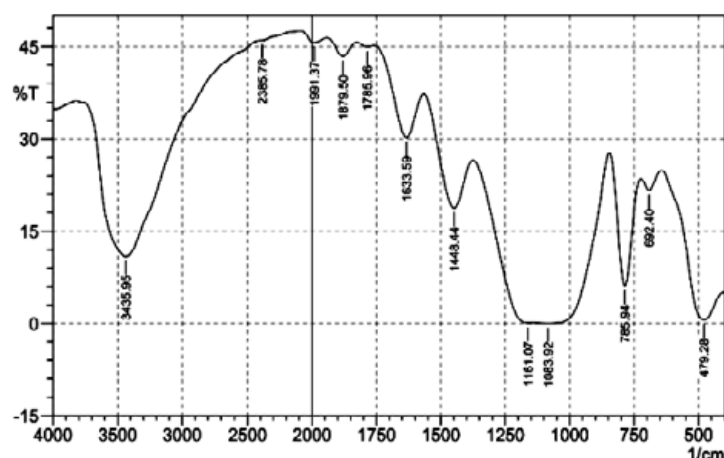


Figure 12: FT-IR spectra of SiO₂ NPs obtained by milling of yellow sand .

FTIR. The results showed that the SiO₂ NPs have spherical shape and with crystalline structure.

References

- Datta MK, Pabi SK, Murty BS (2000) Thermal stability of nanocrystalline Ni silicides synthesized by mechanical alloying. *Mater. Sci.Eng.* 284: 219-225.
- Gleiter H (1989) Nanocrystalline materials *Prog. Mater. Sci* 33: 223-315.
- Murray CB, Sun S, Doyle H, Bitley T (2001) Monodisperse 3d Transition Metal (Co, Ni, Fe) Nanoparticles and Their Assembly into Nanoparticle Superlattices. *MRS Bull* 26: 981-985 .
- Karch J, Birringer R, Gleiter H (1987) Ceramics ductile at low temperature *Nature* 300: 556-558.
- Siegel RW, Hahn H, Ramasamy S, Zongquan L, Ting L, et al. (1988) Structure and Properties of Nanophase TiO₂. *J. Phys. Colloq* 49: 68-686.
- Jafarzadeh M, Rahman IA, Sipaut CS (2009) Synthesis of silica nanoparticles by modified sol-gel process: the effect of mixing modes of the reactants and drying techniques. *J Sol-Gel Sci Technol* 50: 328-336.
- Zawrah MF, EL-Kheshen AA, Abd-EL-aal H M (2009) Facile And Economic Synthesis of Silica Nanoparticles *J Ovonic Resear* 5: 129-133.
- Kota SR, Khalil E, Tsutomu K, Kazumi M, Keisuke M (2005) A novel method for synthesis of silica nanoparticles. *J Colloid Interf. Sci* 289: 125-131.
- Sung KP, Ki DK, Hee TK (2002) *Colloids & Surfaces A: Physicochemical and Engineering Aspects* 197: 7-17
- Anna BC, Federica B, Anna MF, Bonaventura F, Cristina L (2006) *Powder Technology* 167: 45-48.
- Werner S, Arthur F (1968) Controlled growth of monodisperse silica spheres in the micron size range. *J colloid and interface science* 26: 62-69.
- Boguch GH, Tracy MA, Zukoski CF (1988) Preparation of Monodisperse Silica Particles: Control of Size and Mass Fraction. *J Non-Crystalline Solids* 104: 95-106.
- Abarkan I, Doussineau T, Smaïhi M (2006) Tailored macro/microstructural properties of colloidal silica nanoparticles via microemulsion preparation *Polyhedron* 25: 1763-1770.
- Gan LM, Zhang K, Chew C.H (1996) Preparation of silica nanoparticles from sodium orthosilicate in inverse microemulsions. *Colloids and Surfaces A: Physicochem Engineer Asp* 110: 199-206.
- Zaky RR, Hessien MM, El-Midany AA, Khedr MH, Abdel-Aal EA, et al. (2008) Preparation of silica nanoparticles from semi-burned rice straw ash. *Powder Techn* 185: 31-35.
- Zhao M, L Zheng L, Bai X, Li N, Yu L (2009) Fabrication of silica nanoparticles and hollow spheres using ionic liquid microemulsion droplets as templates. *Colloids and Surfaces A: Physicochem. Eng. Aspects* 346: 229-236.
- Gao GM, Zou HF, Gan SC, Liu ZJ, An BC, et al. (2009) Preparation and properties of silica nanoparticles from oil shale ash. *Powder Techn* 191: 47-51.

18. Hee DJ (2001) Experimental study of synthesis of silica nanoparticles by a bench-scale diffusion flame reactor. *Powder Techn* 119: 102–108.
19. Patil A, Chirmade UN, Trivedi V, Lamprou DA, Urquhart A, et al. (2011) Encapsulation of Water Insoluble Drugs in Mesoporous Silica Nanoparticles using Supercritical Carbon Dioxide. *J Nanomed & Nanotechnol* 2:111.
20. Morohashi S, Sawahara Y (1973) *J. Soc. Mater. Sci Jpn*, 22689–22692.
21. Brinker CJ, Scherer GW (1990) *Sol–gel Science. The Physics and Chemistry of Sol–gel Processing*, Academic, New York, 581.
22. Socrates G (2001) *Infrared and Raman Characteristic Group Frequencies: Tables and Charts*, third ed, Wiley, 245.
23. Duran A, Fernandez-Navarro JM, Casariego P, Joglar A (1986) Optical properties of glass coatings containing Fe and Co. *J. Non-Cryst. Solids* 82: 69.
24. Bertoluzza A, Fagnano C, Morelli MA, Gottardi V, Guglielmi M (1982) Raman and infrared spectra on silica gel evolving toward glass. *J Non-Cryst.Solids* 48: 117-128.
25. Gopal NO, Narasimhulu KV, Rao JL (2004) EPR, optical, infrared and Raman spectral studies of Actinolite mineral. *Acta Part A* 60: 2441-2448.